Supplementary Figure. 1

Root phenotyping of Mediator mutants

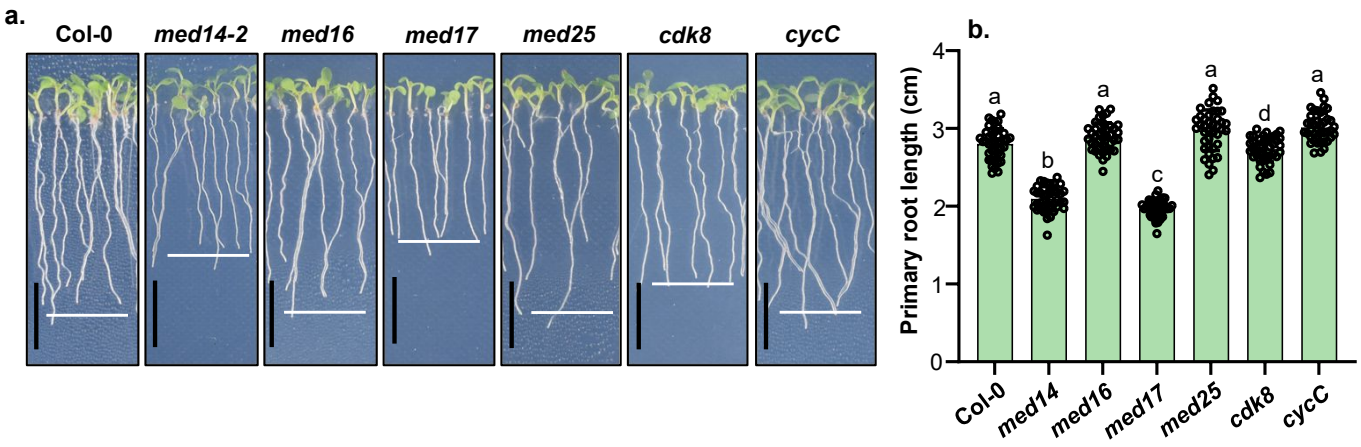

S1: Involvement of Mediator subunits in the maintenance of RSA. a, Representative image showing the phenotype of 10th-day-old seedlings of Col-0, *med14-2*, *med16*, *med17*, *med25*, *cdk8*, and *cycC*, grown on ½ MS medium. **b,** Graphical representation showing the primary root length of 10th-day-old roots of Col-0 and the mutants of Mediator subunits. Data shown in the graph represents the average of three independent biological replicates containing at least 20 seedlings. Bar plots represent the mean value and the black circles represent the individual values. Statistical significance was determined using a one-way ANOVA followed by Tukey's honestly significant difference (HSD) post hoc test. Statistical significance was determined by a P-value of 0.05 or lower ($P \leq 0.05$), while P-values greater than 0.05 ($P > 0.05$) were considered non-significant and depicted with alphabets. Scale bar=100 mm.

Supplementary Figure. 2

Preparation of RNAi lines of *med14* mutants and transcript level of *MED14* in RNAi and T-DNA lines

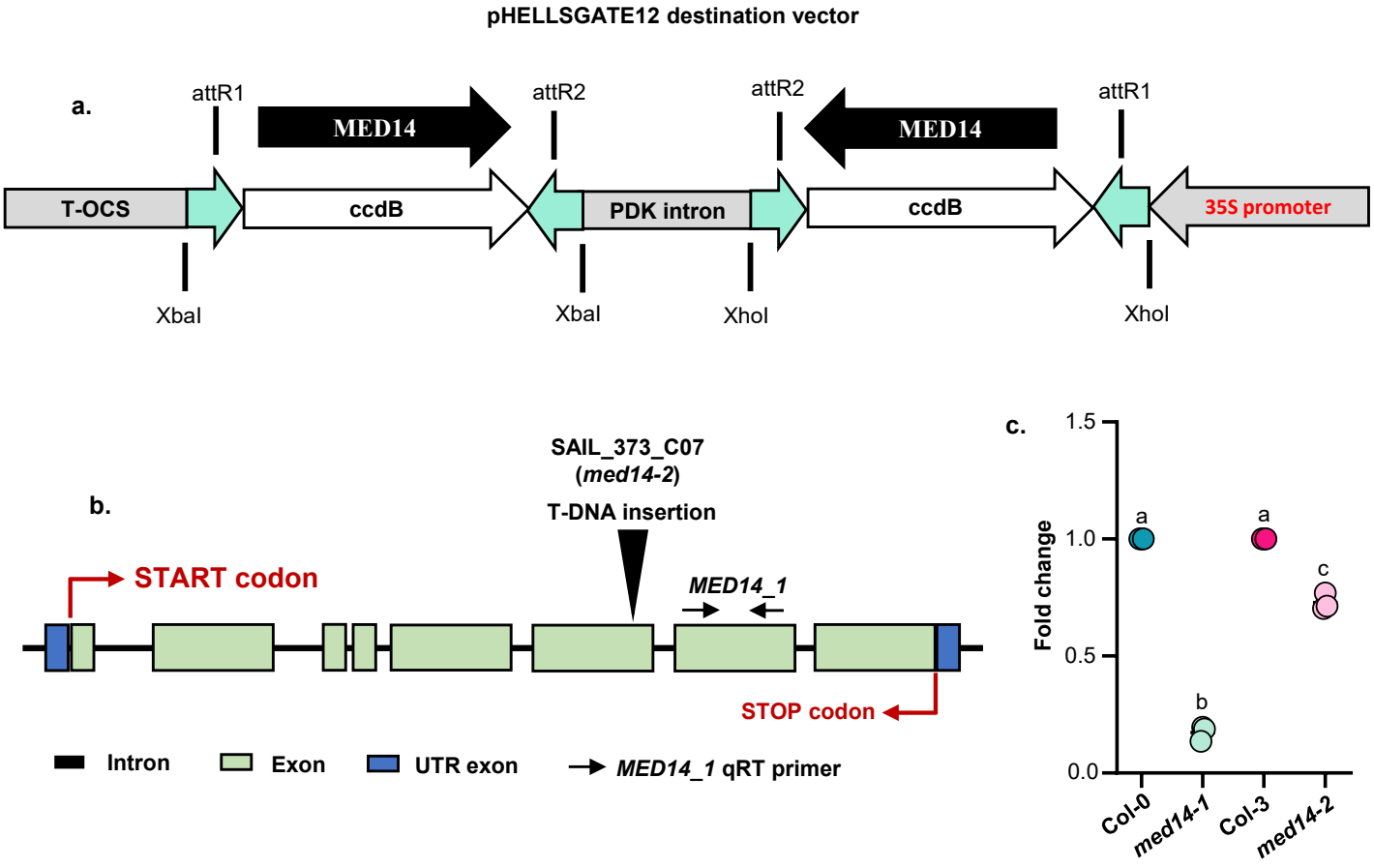

S2: Confirmation of *med14* mutant lines. a, Plasmid design for *MED14* RNAi line. **b,** T-DNA insertion mutant of *med14* (named as *med14-2*) showed the insertion at the end of the 6th exon. **c,** Confirmation of *MED14* expression in 6th-day-old seedlings of wild-type and *med14* mutants by using the *MED14* primers designed from the 7th exon of the *MED14* gene. Gene expression values were calculated as fold change ($2^{-\Delta\Delta CT}$). qRT-PCR analysis was performed with three independent biological replicates (n=3) and repeated the experiment thrice. Scatter dot plots represent individual values of biological replicates and error bars denote standard deviation (SD). Statistical significance was determined using a one-way ANOVA followed by Tukey's honestly significant difference (HSD) post hoc test. Statistical significance was determined by a P-value of 0.05 or lower ($P \leq 0.05$), while P-values greater than 0.05 ($P > 0.05$) were considered non-significant and depicted with alphabets.

Supplementary Figure. 3

Phenotypic characterization of *med14* mutants

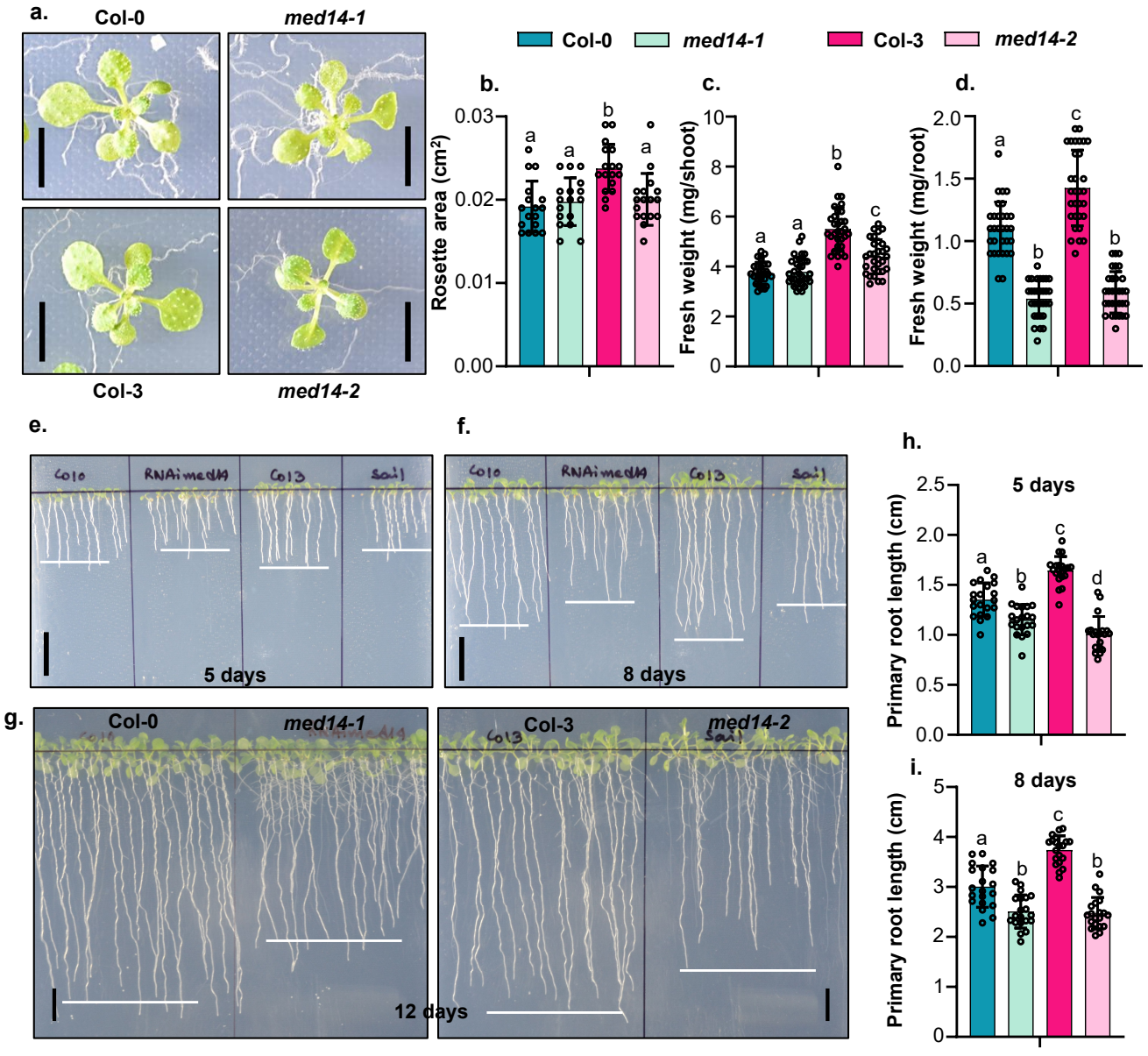

S3: Involvement of MED14 in shoot and root development in Arabidopsis. a, Representative images showing the shoot phenotype of 12th-days-old Col-0, *med14-1*, Col-3, and *med14-2*. **b,** Graph showing the rosette area of wild-types and *med14* mutants. **c and d,** Graph showing the fresh weight of shoot and root per plant. **e-g,** Representative images showing the 5th, 8th, and 12th day old root phenotype of wild-type and *med14* mutants. **h and i,** Graph showing the primary root length of 5th and 8th days old wild-type and *med14* mutant. Data shown in the graph represents the average of three independent biological replicates containing at least 20 seedlings. Rosette area was measured by using Image J software. Bar plots represent the mean value and the black circles represent the individual values. Statistical significance was determined using a one-way ANOVA followed by Tukey's honestly significant difference (HSD) post hoc test. Statistical significance was determined by a P-value of 0.05 or lower ($P \leq 0.05$), while P-values greater than 0.05 ($P > 0.05$) were considered non-significant and depicted with alphabets. Scale bar=100 mm.

Supplementary Figure. 4

Phenotypic characterization of lateral roots in *med14* mutants

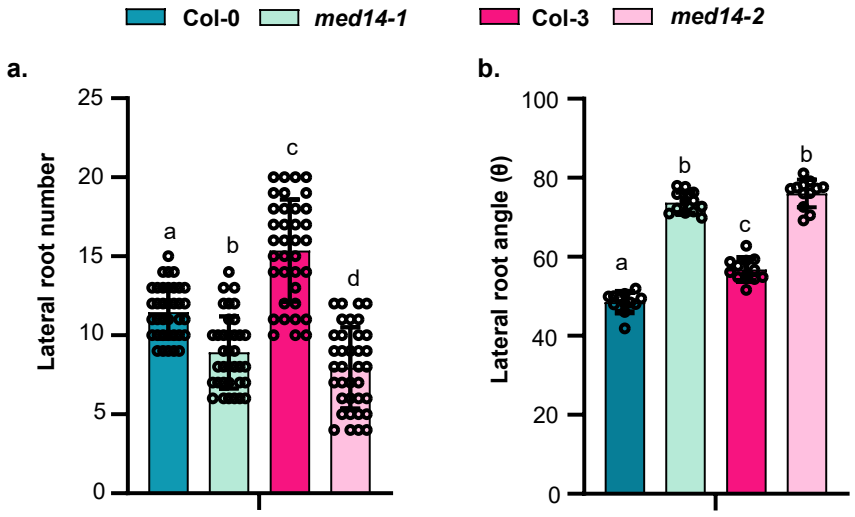

S4: MED14 regulates the lateral root formation in Arabidopsis root. a, Graph showing the number of lateral roots in 12th-day-old seedlings of wild-type and *med14* mutants. **b,** Graph showing the lateral root angle in 12th-day-old wild-type and *med14* mutants. Data shown in the graph represents the average of three independent biological replicates containing at least 15 seedlings. Bar plots represent the mean value and the black circles represent the individual values. Statistical significance was determined by using a one-way ANOVA followed by Tukey's honestly significant difference (HSD) post hoc test. Statistical significance was determined by a P-value of 0.05 or lower ($P \leq 0.05$), while P-values greater than 0.05 ($P > 0.05$) were considered non-significant and depicted with alphabets.

Supplementary Figure. 5

Cell division in *med14* mutants and complementation lines

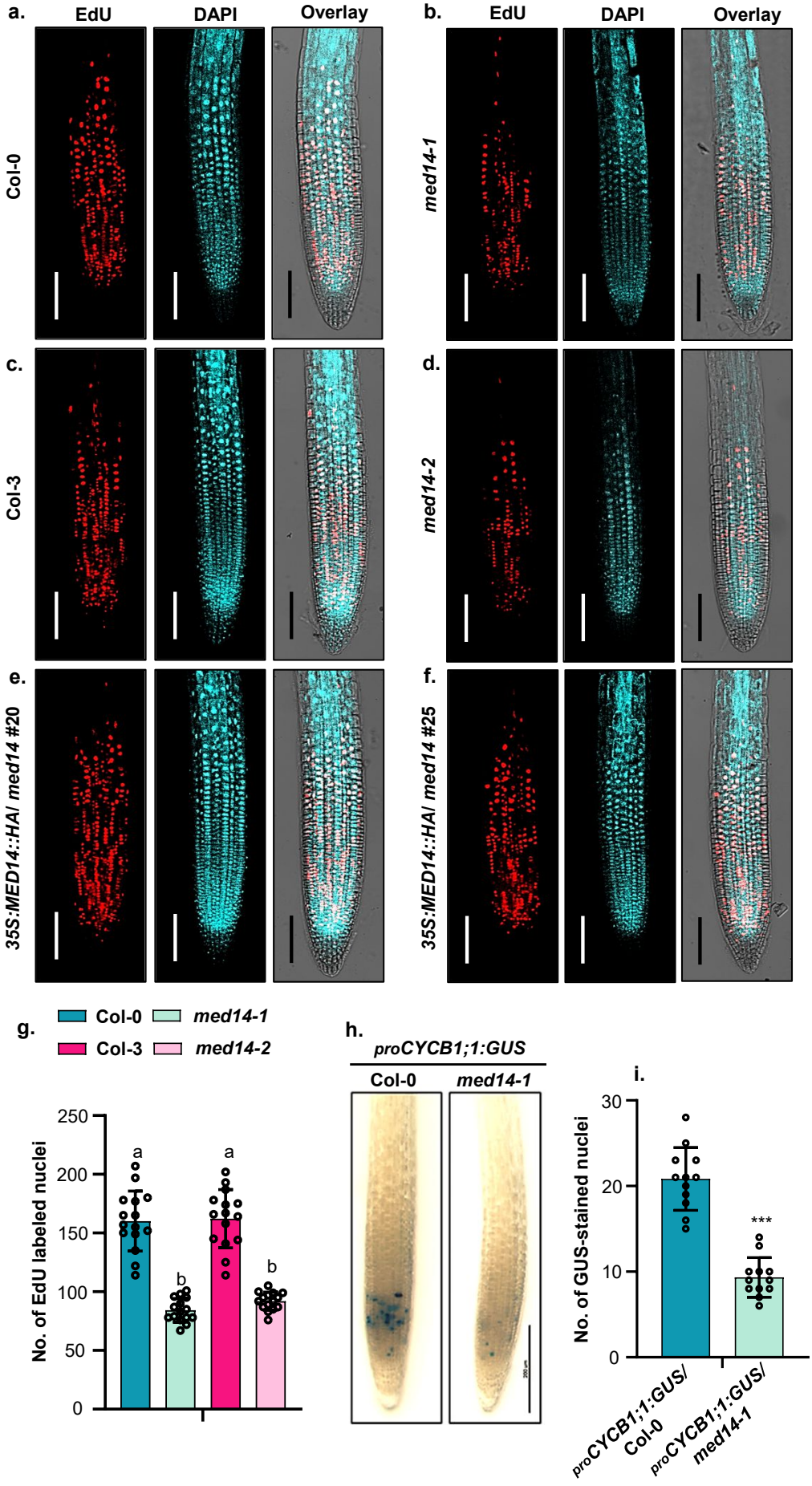

S5: MED14 regulates cell division at the root apical meristem. a-f, Confocal images showing the 6th-days-old roots of wild-type and *med14* and complementation lines (*35S:MED14::HA*/*med14* #20, #25), stained with EdU followed by DAPI. **g,** Graph showing the number of EdU-labeled nuclei. **h,** Stereomicroscopic image showing the GUS expression of $_{pro}$*CYCB1;1:GUS* line in Col-0 and *med14-1* background. **i,** Graphical representation showing the number of GUS-stained nuclei. Data shown in the graphs represents the average of three independent biological replicates containing at least 15 seedlings for (a-g) and 12 seedlings for (h-i). Bar plots represent the mean value and the black circles represent the individual values. Error bars denote standard deviation (SD). Statistical significance was determined using a one-way ANOVA followed by Tukey's honestly significant difference (HSD) post hoc test. Statistical significance was determined by a P-value of 0.05 or lower ($P \leq 0.05$), while P-values greater than 0.05 ($P > 0.05$) were considered non-significant (ns) and depicted with alphabets. Statistical differences have also been depicted by P value $P<0.0005$ represented with asterisks (***) as assessed by student's t-test (i). Scale bar=100 μm (a-f), 200 μm (h).

Supplementary Figure. 6

Characterization of *35S:MED14:HA/med14* complementation lines

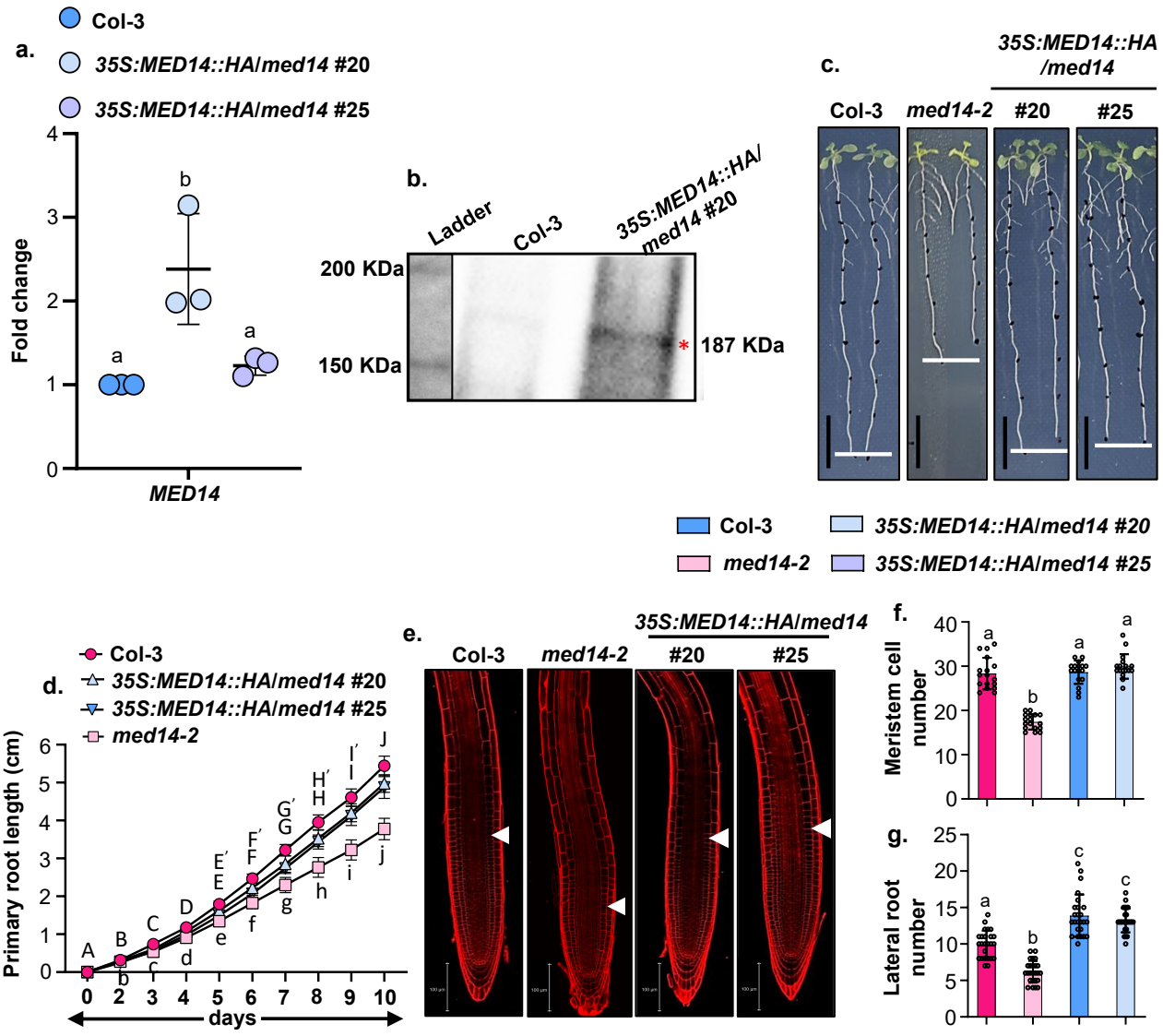

S6: Characterization of the complementation lines of MED14. a, Scatter dot plot showing the transcript level of *MED14* in the roots of Col-3 and MED14 complemented lines (*35S:MED14::HA*/*med14* #20, and #25). **b,** Western blot detection of 6-days-old Col-3, *35S:MED14::HA*/*med14* #20 line. **c,** Representative images showing the root phenotype of 10^{th}-day-old Col-3, *med14-2*, *35S:MED14::HA/med14* #20, and #25 lines. **d,** Line graph showing the primary root length of 10^{th}-day-old Col-3, *med14-2*, and MED14 complementation lines. **e,** Confocal images showing the cellular organization in PI-stained roots of Col-3, *med14-2,* and MED14 complementation lines. Arrows showing the end of meristematic zone. **f,** Graph showing the meristem cell number in the Col-3, *med14-2*, and MED14 complementation lines. Cell numbers were calculated from the confocal images. **g,** Graph showing the lateral root number of 10-day-old roots of wild-type, *med14-2* mutant, and MED14-complemented lines. Gene expression values were calculated as Fold change ($2^{-\Delta\Delta CT}$). qRT-PCR analysis was performed with three independent biological replicates (n=3) and repeated the experiment thrice. Scatter dot plots represent individual values of biological replicates and error bars denote standard deviation (SD). Data shown in the graph represents the average of three independent biological replicates containing at least 15 seedlings. Bar plots represent the mean value and the black circles represent the individual values. Statistical significance was determined by using a one-way ANOVA followed by Tukey's honestly significant difference (HSD) post hoc test. Statistical significance was determined by a P-value of 0.05 or lower ($P \leq 0.05$), while P-values greater than 0.05 ($P > 0.05$) were considered non-significant and depicted with alphabets. For (d) capital letters (A-J) denote the significance of wild-types and small letters (a-j) denote the significance of mutants. And the (E'-J') qualified the significance test in complementation lines compared to wild-type and *med14-2* mutant. Scale bar=100 mm (c), 100 µm (e).

Supplementary Figure. 7

Characterization of *MED14$_{pro}$:MED14::YFP* line

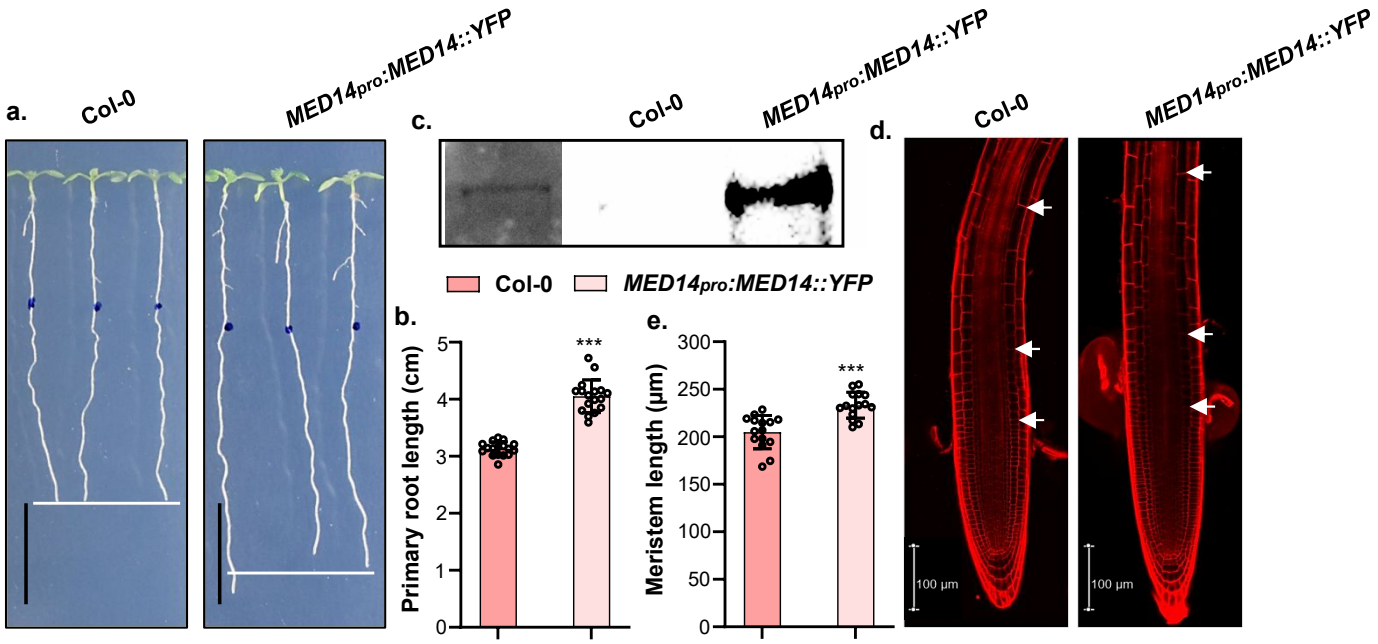

S7: Characterization of *MED14$_{pro}$:MED14::YFP* line. a, Representative image showing the root phenotype of 12th-day-old roots of Col-0 and *MED14$_{pro}$:MED14::YFP*. **b,** Graph showing the primary root length of Col-0 and *MED14$_{pro}$:MED14::YFP* measured by Image J software. **c,** Western blot detection of 6th-days-old seedlings of Col-0 and *MED14$_{pro}$:MED14::YFP*. **d,** Confocal images showing the cellular organization of Col-0 and *MED14$_{pro}$:MED14::YFP* roots, stained with PI. Arrows showing the end of meristematic, transition, and elongation zones respectively. **e.** Graph showing the meristem length of PI-stained roots of Col-0 and *MED14$_{pro}$:MED14::YFP*. Meristem length was measured using Image J software. Data shown in the graph represents the average of three independent biological replicates containing at least 15 seedlings. Bar plots represent the mean value, and the black circles represent the individual values. Statistical significance has also been depicted by P value P<0.05, <0.005, <0.0005 represented with *, **, and *** respectively, represented with (*) asterisks as assessed by Student's t-test. Scale bar=100 mm (a), 100 µm (d).

Supplementary Figure. 8

Transcriptomic analysis of *med14* mutant

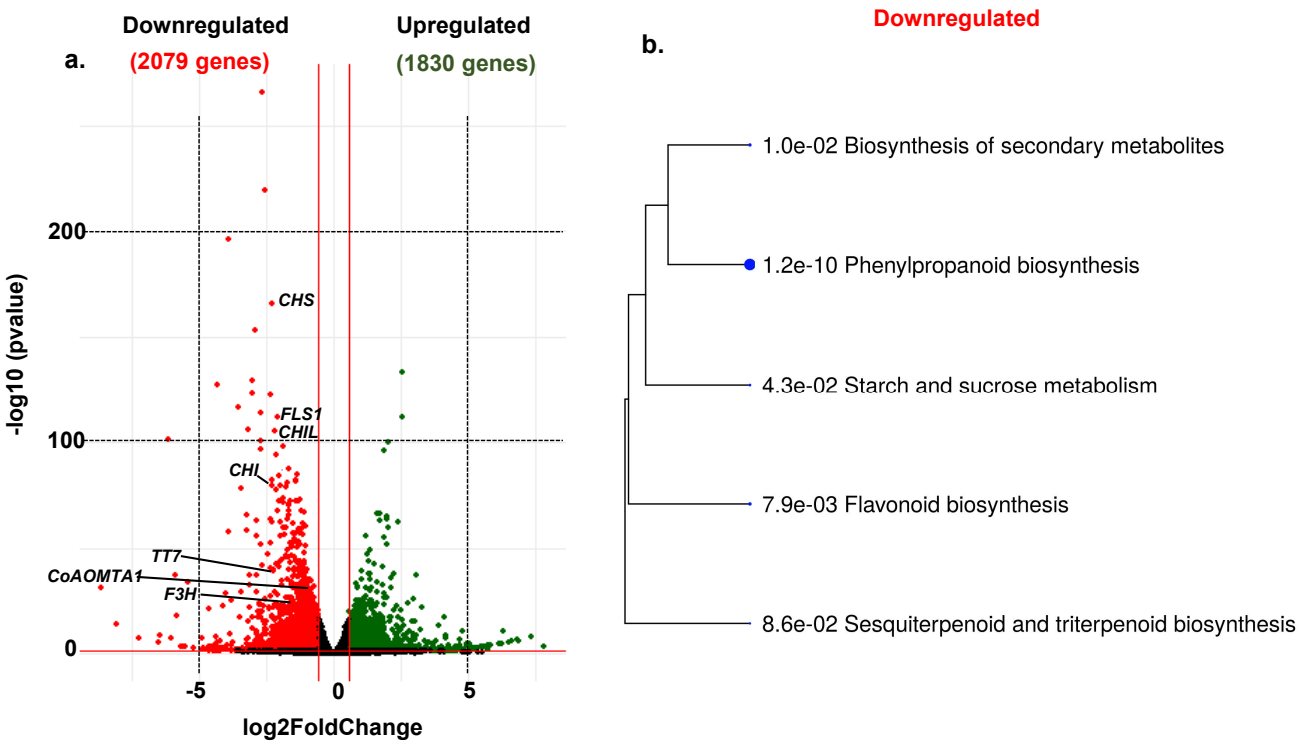

S8: Transcriptome analysis of *med14* mutant roots. a, Volcano plot showing total differentially expressed genes (DEGs) in the roots of 6-day-old *med14-1* roots as compared to Col-0. **b,** GO enrichment analysis showing the enriched pathways of downregulated genes in *med14-1* mutant compared to Col-0. GO enrichment analysis was done by using ShinyGO 8.0 tools. Volcano plots were generated by using R software.

Supplementary Figure. 9

Characterization of *HY5pro:HY5::GFP* lines in Col-0 and *med14-1* background

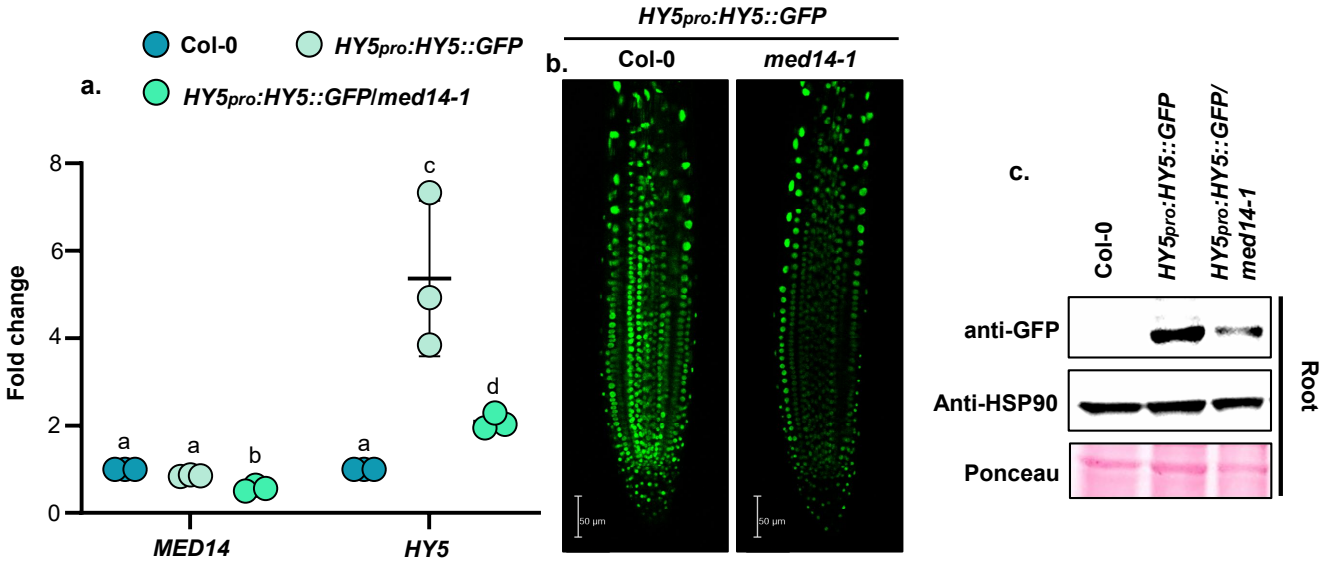

S9: Characterization of *HY5$_{pro}$:HY5::GFP* lines. **a,** Gene expression of *MED14* and *HY5* in the 6th-days-old seedlings of Col-0, *HY5$_{pro}$:HY5::GFP*/Col-0, and *HY5$_{pro}$:HY5::GFP/med14-1* line by qRT-PCR. **b,** Confocal images showing the protein level of HY5-GFP in 6th-day-old roots of *HY5$_{pro}$:HY5::GFP*/Col-0 and *HY5$_{pro}$:HY5::GFP/med14-1* lines. **c,** Western blot detection in 6th-day-old root tissues of Col-0, *HY5$_{pro}$:HY5::GFP* in Col-0 and *med14-1* background independently. Gene expression values were calculated as Fold change ($2^{-\Delta\Delta CT}$). qRT-PCR analysis was performed with three independent biological replicates (n=3) and repeated the experiment twice. Scatter dot plots represent individual values of biological replicates and error bars denote standard deviation (SD). Data shown in the graph represents the average of three independent biological replicates containing at least 15 seedlings. Bar plots represent the mean value, and the black circles represent the individual values. Statistical significance was determined by using a one-way ANOVA followed by Tukey's honestly significant difference (HSD) post hoc test. Statistical significance was determined by a P-value of 0.05 or lower ($P \leq 0.05$), while P-values greater than 0.05 ($P > 0.05$) were considered non-significant and depicted with alphabets. Scale bar=50 µm (B).

Supplementary Figure. 10

Prediction for the binding of MED14 and HY5 by molecular docking

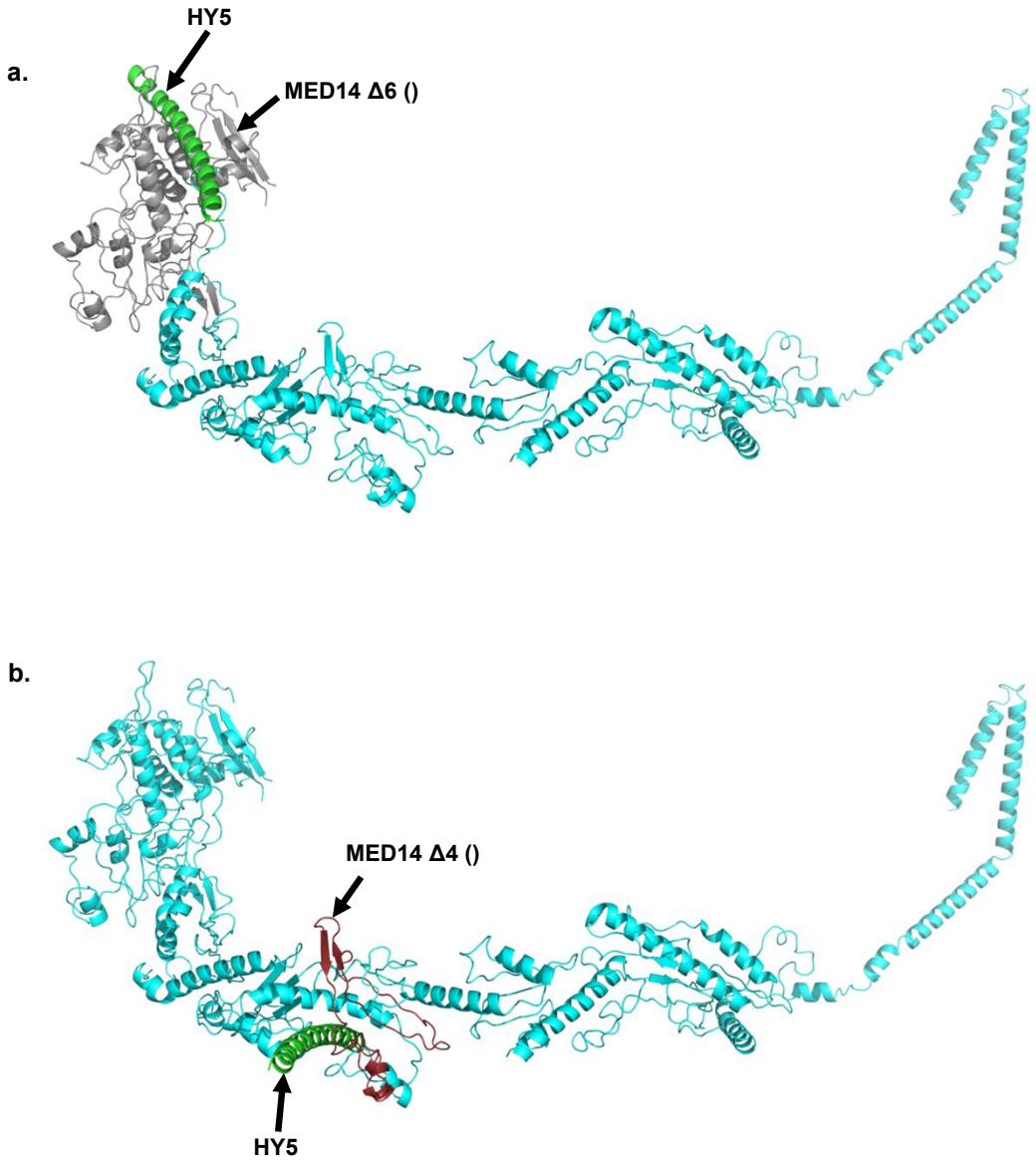

S10: Protein-protein docking of HY5 and MED14. a, Top hit docking pose shows the binding of HY5 (green) within the **Δ**6 region (grey) of MED14. **b,** Second top hit docking pose shows the binding of HY5 (green) within the **Δ**4 region (grey) of MED14.

Supplementary Figure. 11

Interaction of MED14 and HY5 by BiFC

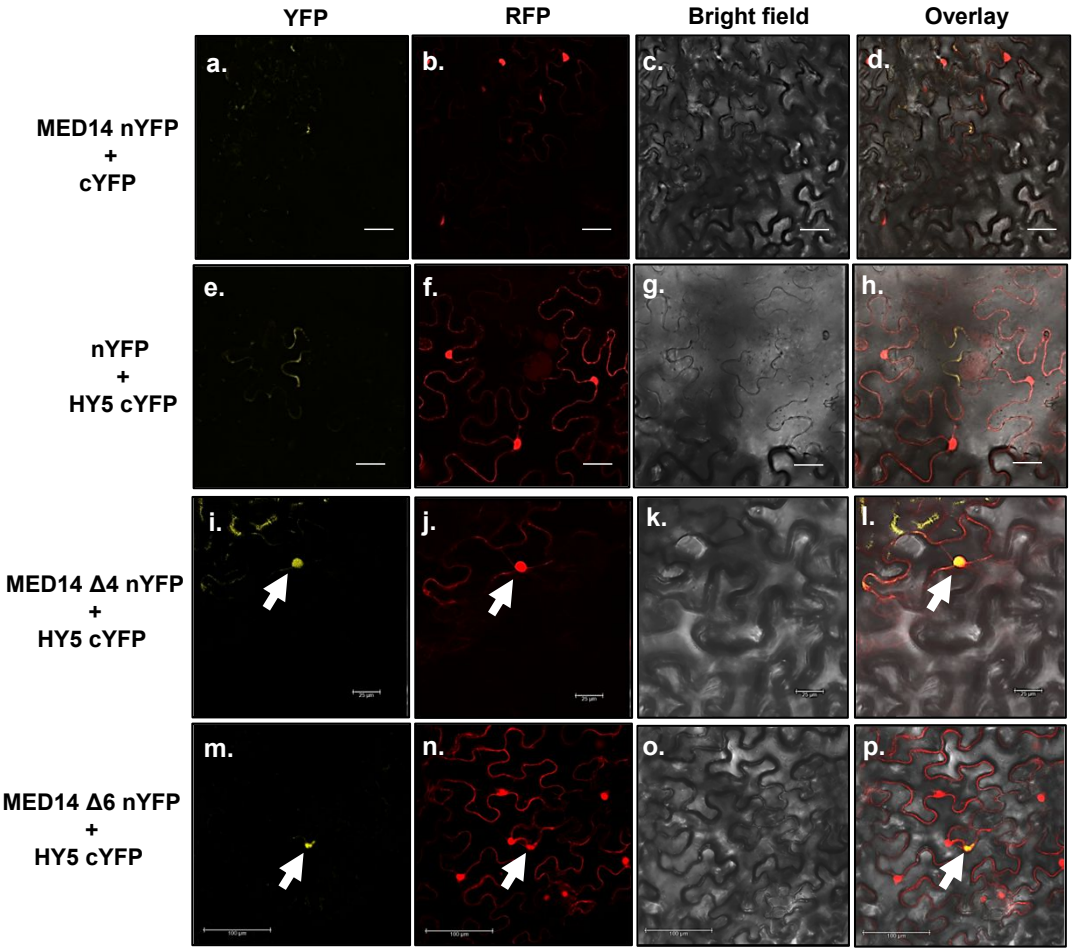

S11: MED14 interact with HY5 by BiFC. a-p, The YFP and RFP signal was observed under confocal microscope in *Nicotiana benthamiana* leaves that co-transformed with pDEST-VYNE MED14 (Δ4 and Δ6) and pDEST-VYCE HY5 and their respective vector controls. Merged images showed the co-localization of YFP with the nucleus marker (Red colored/RFP), showing the interaction of the two proteins. Scale Bar= 25µm (a-l), 100µm (m-p)

Supplementary Figure. 12

Phenotype of cell numbers in *med14-1*, *hy5,* and double mutants

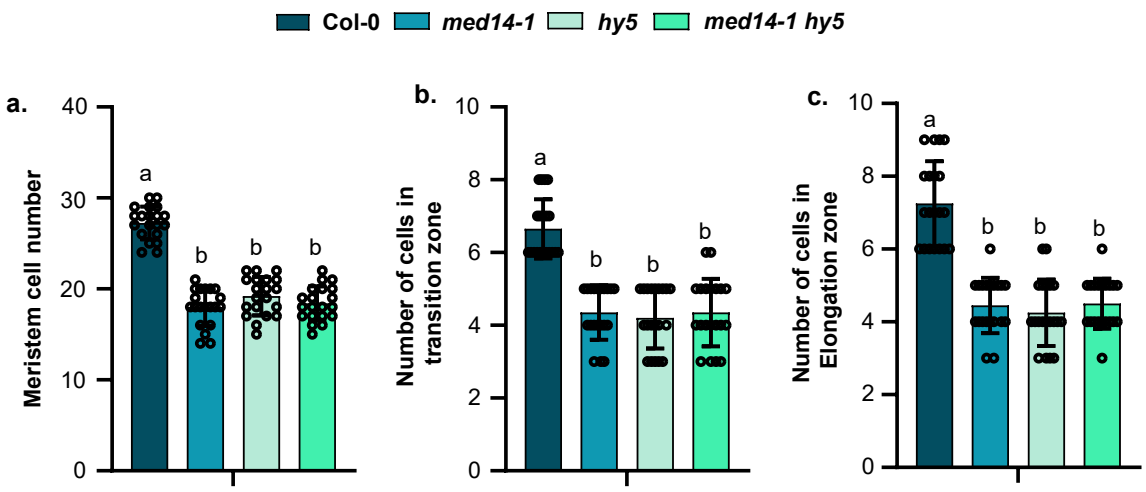

S12: MED14 and HY5 regulate cell numbers in the root. a-c, Graphs representing the number of cells in meristematic, transition, and elongation zones in the roots of Col-0, *med14-1*, *hy5*, and double mutants, respectively. Data shown in the graphs represents the average of three independent biological replicates containing at least 20 seedlings. Bar plots represent the mean value, and the black circles represent the individual values. Error bars denote standard deviation (SD). Statistical significance was determined using a one-way ANOVA followed by Tukey's honestly significant difference (HSD) post hoc test. Statistical significance was determined by a P-value of 0.05 or lower ($P \leq 0.05$), while P-values greater than 0.05 ($P > 0.05$) were considered non-significant (ns) and depicted with alphabets.

Supplementary Figure. 13

Cell elongation and cell division of *med14-1*, *hy5,* and double mutants

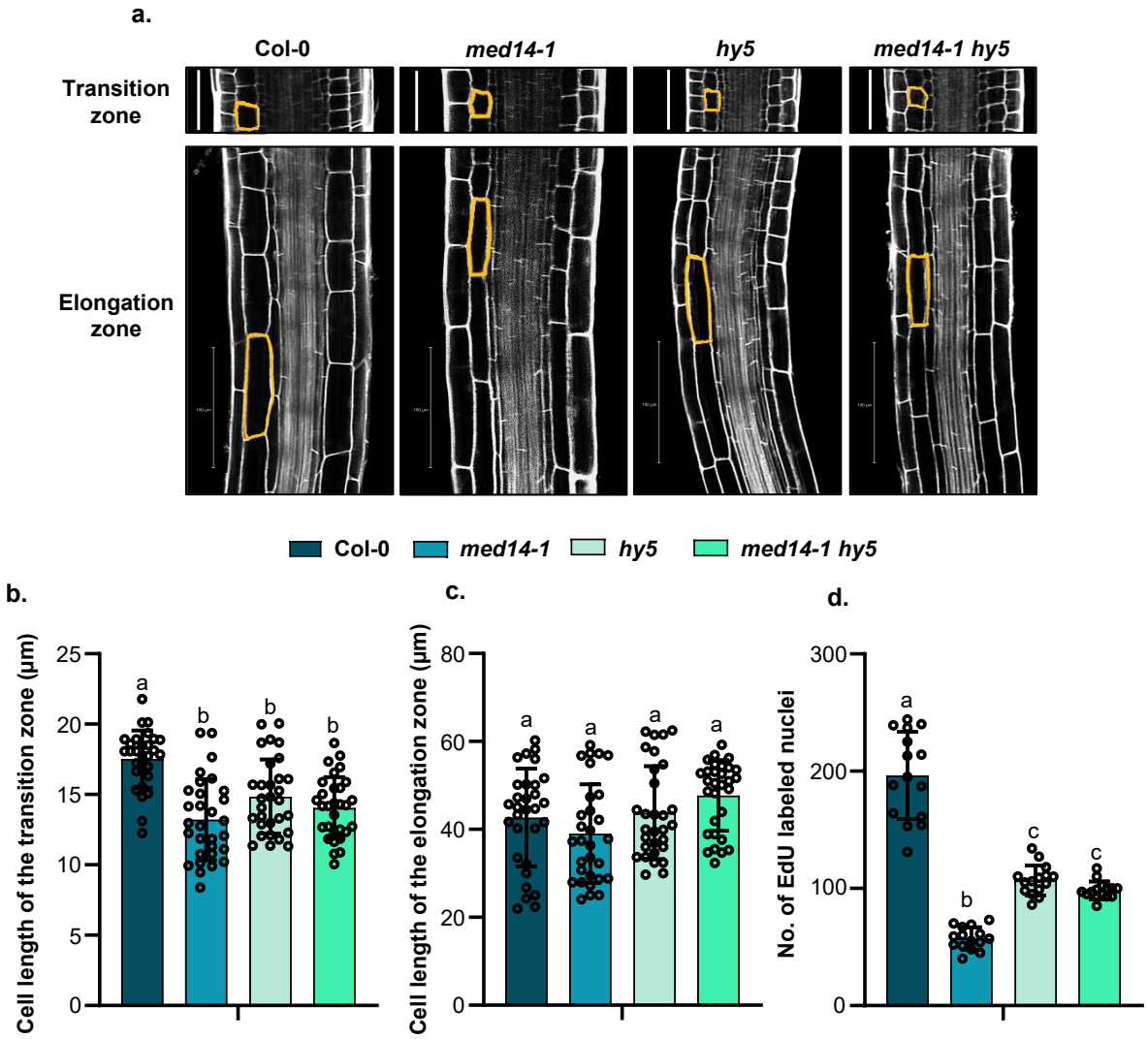

S13: Involvement of HY5 in cell elongation. a, Confocal images represented PI-stained roots showing the length of the cells in transition and elongation zones. Yellow marks showed the individual cells in the different zones. **b and c,** Graphs showing the length of the cells in transition and elongation zone of Col-0, *med14-1*, *hy5,* and *med14-1 hy5* roots. Cell length was calculated from the confocal image. **d,** Graph showing the number of EdU-labelled nuclei in the Col-0, *med14-1*, *hy5*, and *med14-1 hy5* mutant roots. Data shown in the graph represents the average of three independent biological replicates containing at least 20 seedlings. Bar plots represent the mean value, and the black circles represent the individual values. Statistical significance was determined by using a one-way ANOVA followed by Tukey's honestly significant difference (HSD) post hoc test. Statistical significance was determined by a P-value of 0.05 or lower ($P \leq 0.05$), while P-values greater than 0.05 ($P > 0.05$) were considered non-significant and depicted with alphabets. Scale bar=100 µm.

Supplementary Figure. 14

MED14 and HY5 commonly regulate flavonoid biosynthesis in root

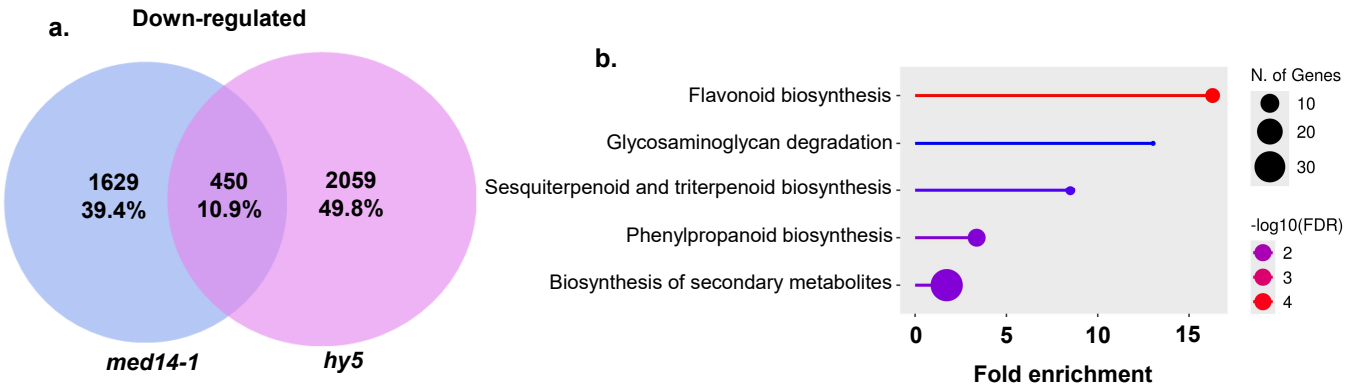

S14: MED14 and HY5 regulate cell division through modulating flavonoid biosynthesis. **a,** Venn diagram showing the downregulated genes common in both the mutant roots of *med14-1* and *hy5*. Venn diagram was generated by using Venny 2.0 tool. **b,** GO enrichment analysis of commonly downregulated genes showing the enriched pathways in both *med14-1* and *hy5* roots. GO enrichment analysis were performed using the ShinyGO 8.0 tool. Colors depicted -log10 (FDR). Bubble size depicted the number of genes.

Supplementary Figure. 15

MED14 complementation reduces ROS homeostasis in *med14* roots

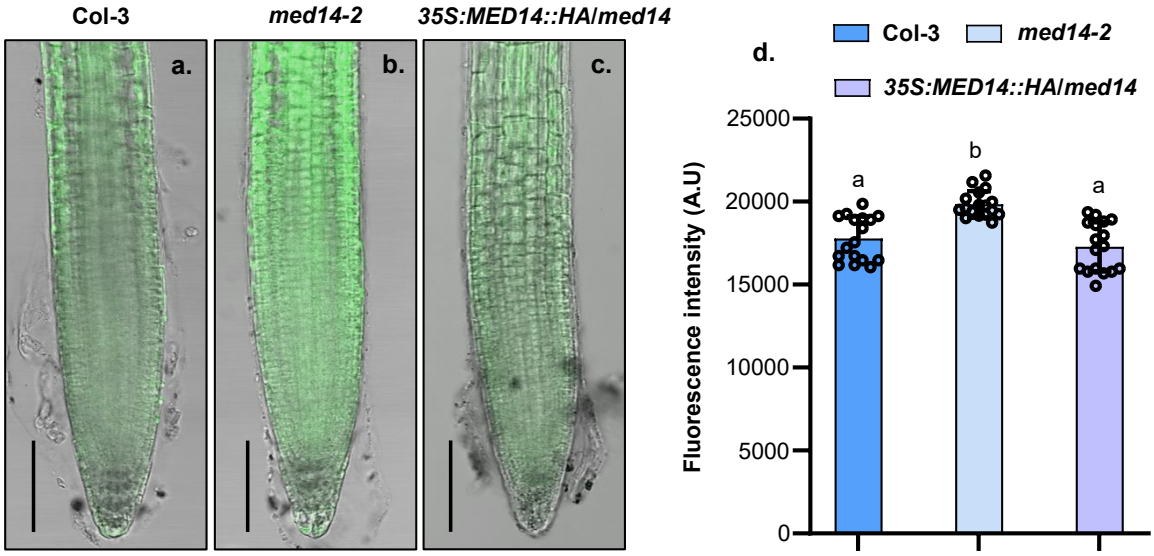

S15: Complementation of MED14 reduces the ROS accumulation in the *med14* root. a-c, Confocal images represent the 6th-days-old roots of Col-0, *med14-2*, and *35S:MED14::HA/med14* #20 line stained with H_2DCFDA. Confocal images are the representative images of at least 15 seedlings. **d,** Graphical representation showing the relative fluorescence intensity of H_2DCFDA stain. Bar plots represent the mean value and the black circles represent the individual values. Error bars denote standard deviation (SD). Statistical significance was determined by using a one-way ANOVA followed by Tukey's honestly significant difference (HSD) post hoc test. Statistical significance was determined by a P-value of 0.05 or lower ($P \leq 0.05$), while P-values greater than 0.05 ($P > 0.05$) were considered non-significant and depicted with alphabets. Scale bar= 100 µm

Supplementary Figure. 16

Exogenous H_2O_2 inhibits primary root growth

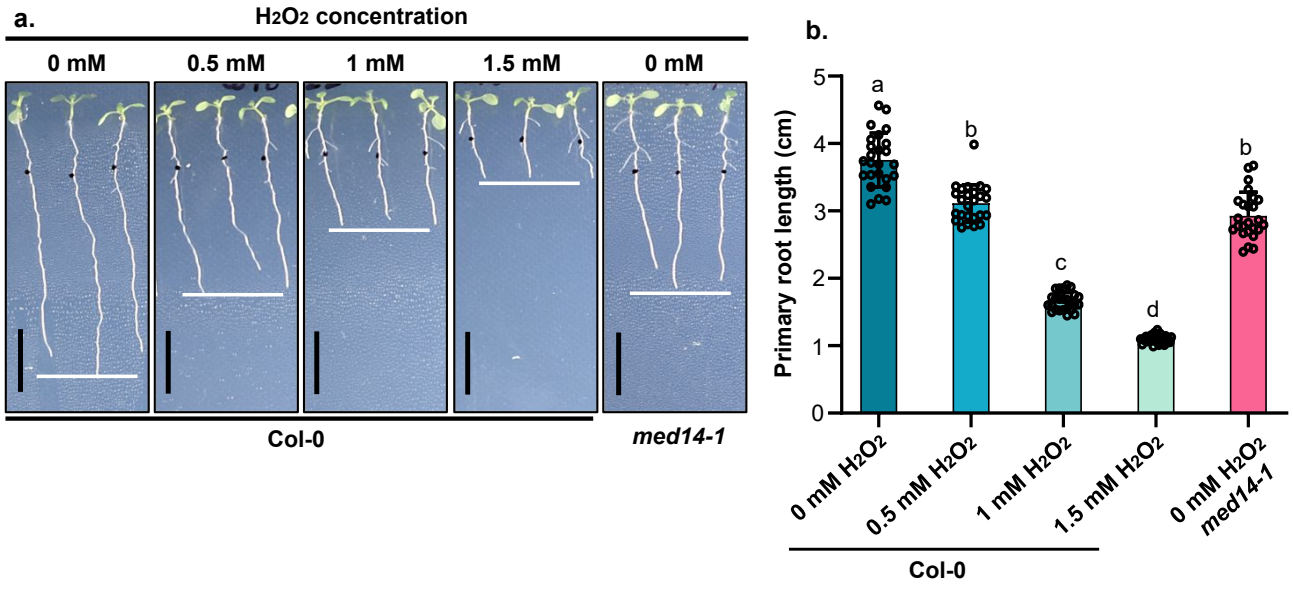

S16: MED14 regulates primary root phenotype through H_2O_2. a, Representative images showing the root phenotype of Col-0 seedlings after the H_2O_2 treatment with different concentrations (0, 0.5, 1, 1.5 mM H_2O_2) and compared with *med14-1* grown on ½ MS medium. **b,** Graph showing the primary root length of Col-0 in H_2O_2 treatment and compared with *med14-1* grown on ½ MS medium. Data shown in the graph represents the average of three independent biological replicates containing at least 20 seedlings. Bar plots represent the mean value and the black circles represent the individual values. Error bars denote standard deviation (SD). Statistical significance was determined by using a one-way ANOVA followed by Tukey's honestly significant difference (HSD) post hoc test. Statistical significance was determined by a P-value of 0.05 or lower ($P \leq 0.05$), while P-values greater than 0.05 ($P > 0.05$) were considered non-significant and depicted with alphabets. Scale bar=100 mm.

Supplementary Figure. 17

Phenotypic characterization of MED14 complementation lines in HU treatment

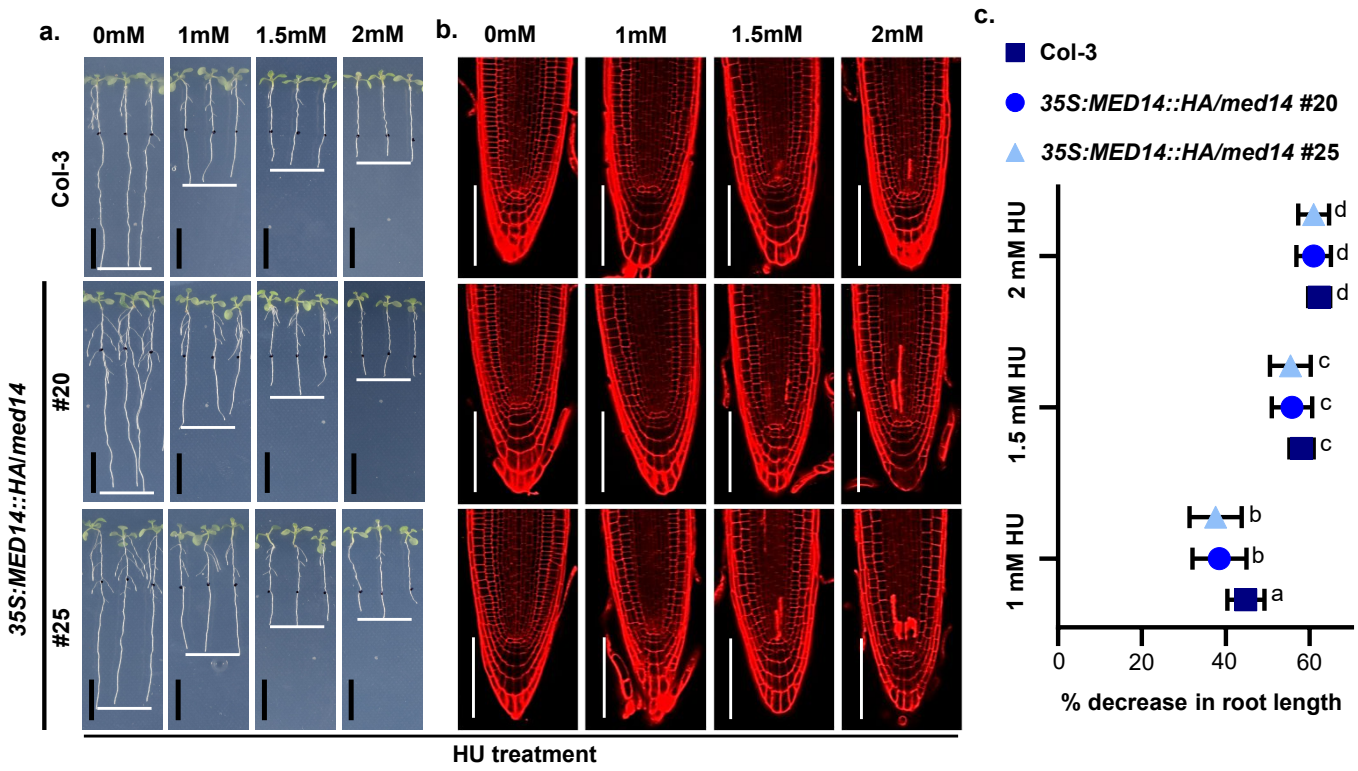

S17: Complementation of MED14 recovers the DDR response in *med14* mutant. a, Representative images showing the root phenotype of Col-3, *35S:MED14::HA/med14* #20 and #25 lines in different concentrations (0, 1, 1.5, 2 mM) of HU treatment. **b,** Confocal images showing the cellular damage in Col-3, *35S:MED14::HA/med14* #20 and #25 roots after HU treatment. Red PI-stained blotches at the root tip denote cell death. **c,** Graphical representation showing the % root length decrease in Col-3 and the MED14 complementation lines in the several concentrations of HU treatment. Data shown in the graph represents the average of three independent biological replicates containing at least 20 seedlings. Bar plots represent the mean value and the black circles represent the individual values. Statistical significance was determined by using a one-way ANOVA followed by Tukey's honestly significant difference (HSD) post hoc test. Statistical significance was determined by a P-value of 0.05 or lower ($P \leq 0.05$), while P-values greater than 0.05 ($P > 0.05$) were considered non-significant and depicted with alphabets. Scale bar=100 mm (a), 100 µm (b).

Supplementary Figure. 18

Comparative analysis of ROS biosynthesis genes in *med14* and *hy5*

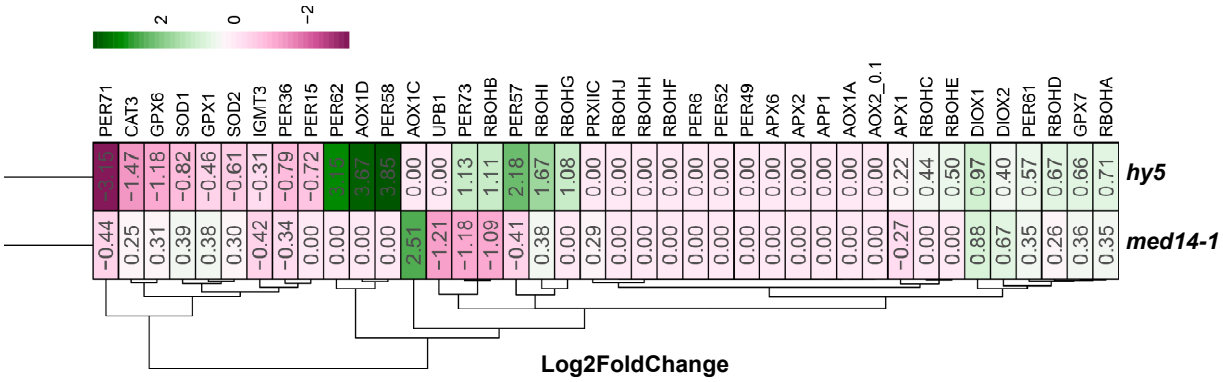

S18: Comparison of ROS biosynthesis genes in transcriptome data of *hy5* and *med14*. Heat map showing the alteration in the expression of ROS biosynthesis genes in *med14-1* and *hy5* mutant. Heat map generated by using R software.

Supplemental figure. 19

Oxidative stress transcriptionally activate DDR response in *med14* and *hy5* mutant

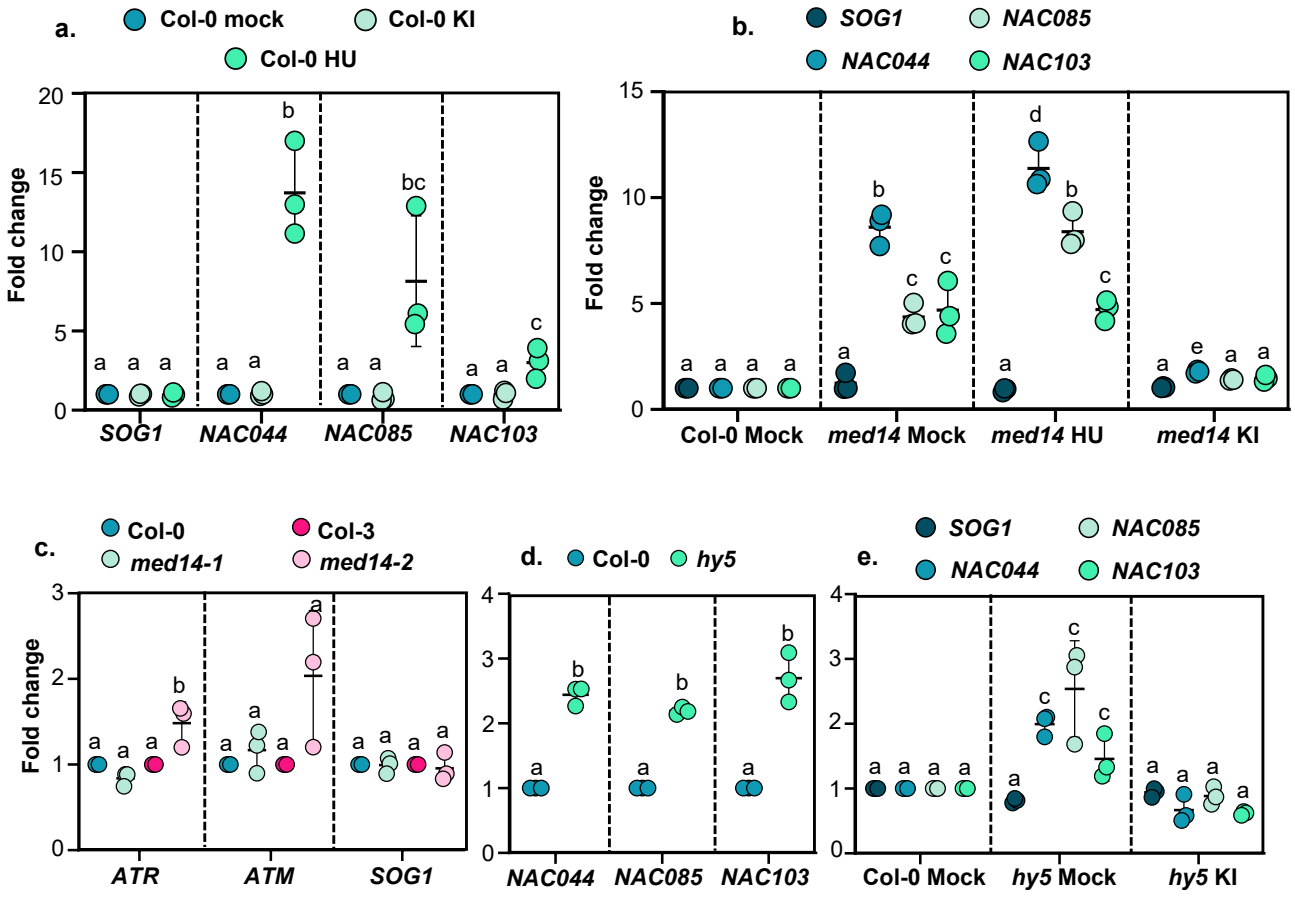

S19: MED14 and HY5 transcriptionally regulate DDR genes to control root elongation in HU treatment. a, Graph showing the gene expression of *SOG1*, *NAC044*, *NAC085,* and *NAC103* in Col-0 roots in response to HU (genotoxic stress) and KI (ROS scavengers) treatment respectively. **b,** Graph showing the expression of *SOG1*, *NAC044*, *NAC085,* and *NAC103* in *med14-1* under mock, HU and KI treatment and compared them with Col-0 in mock. **c,** Graph showing the transcript level of *ATR*, *ATM*, and *SOG1* in wild-type and *med14* mutants roots grown on ½ MS medium. **d,** Graph showing the expression of *NAC044*, *NAC085*, and *NAC103* in Col-0 and *hy5* mutant under normal condition. **e,** Graph representing the expression of *SOG1*, *NAC044*, *NAC085,* and *NAC103* in *hy5* mutant upon KI treatment and compared them Col-0 under mock treatment. Graphs represented with scattered dot plots. Gene expression values were calculated as Fold change ($2^{-\Delta\Delta CT}$). qRT-PCR analysis was performed with three independent biological replicates (n=3). Scatter dot plots represent individual values of biological replicates. Error bars denote standard deviation (SD). Statistical significance was determined using a one-way ANOVA followed by Tukey's honestly significant difference (HSD) post hoc test. Statistical significance was determined by a P-value of 0.05 or lower ($P \leq 0.05$), while P-values greater than 0.05 ($P > 0.05$) were considered non-significant and depicted with alphabets.

Supplementary Figure. 20

Characterization of the root phenotype of *nac044-1*, *nac085-2,* and the double mutants with *med14-1*

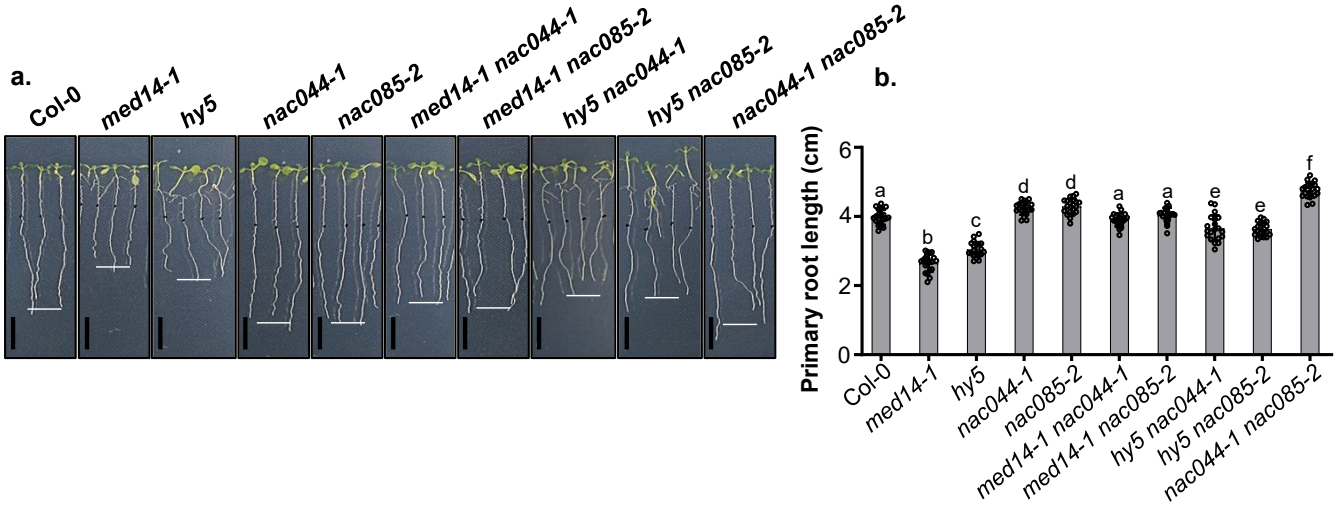

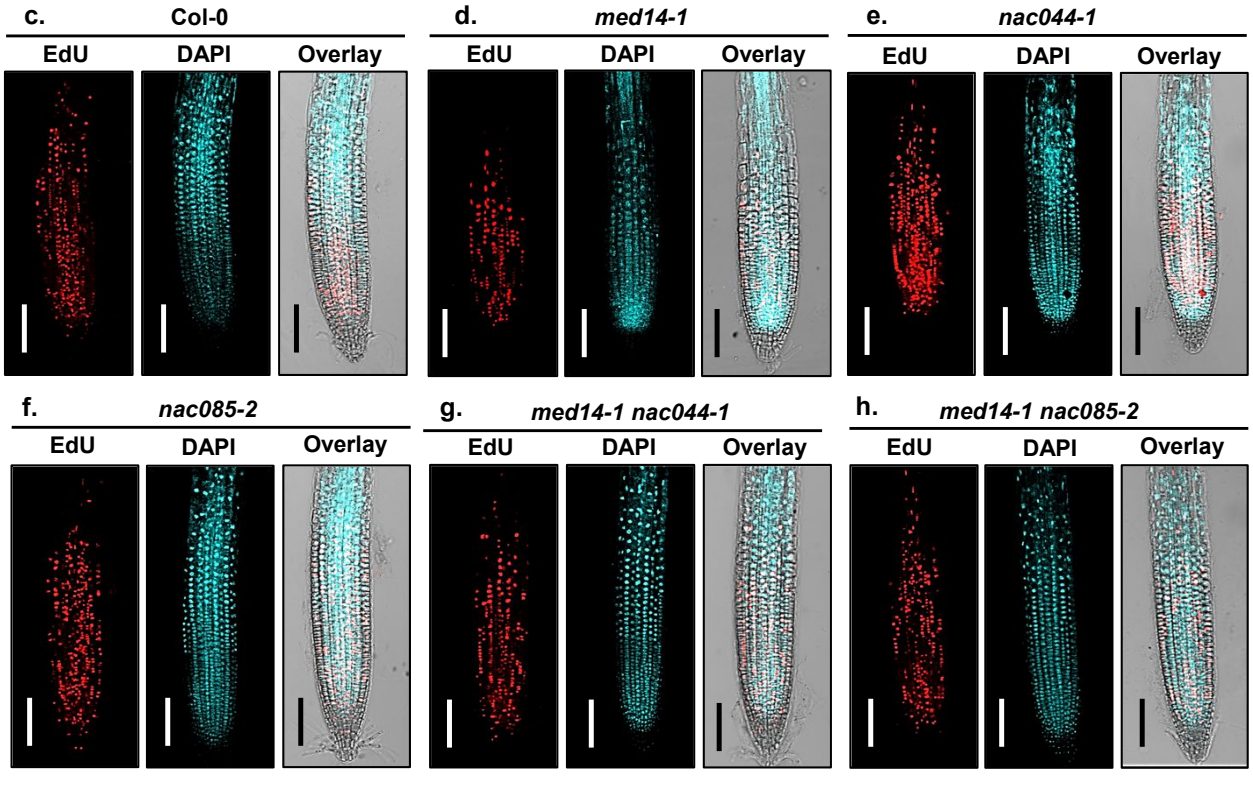

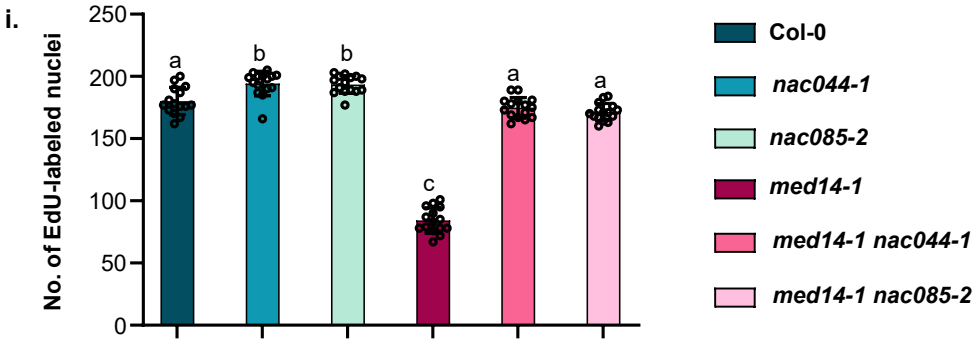

S20: Functional loss of NAC044 and NAC085 complements the root phenotype of *med14* mutant by regulating cell division. a, Representative images showing the root phenotype of Col-0, *med14-1*, *hy5*, *nac044-1*, *nac085-2*, and the double mutants of *med14-1 nac044-1, med14-1 nac085-2, hy5 nac044-1, hy5 nac085-2 and nac044-1 nac085-2*. **b,** Graph showing the primary root length of 10-days-old roots of Col-0, *nac044-1*, *nac085-2*, and all the double mutants. **c-h,** Confocal images showing the EdU labelled nuclei of 6-days-old roots of Col-0, *med14-1*, *nac044-1*, *nac085-2*, and the double mutants of *med14-1 nac044-1* and *med14-1 nac085-2*. **i,** Graphical representation depicted the number of EdU-labelled nuclei. Data shown in the graphs represents the average of three independent biological replicates containing at least 15 seedlings. Bar plots represent the mean value and the black circles represent the individual values. Error bars denote standard deviation (SD). Statistical significance was determined using a one-way ANOVA followed by Tukey's honestly significant difference (HSD) post hoc test. Statistical significance was determined by a P-value of 0.05 or lower ($P \leq 0.05$), while P-values greater than 0.05 ($P > 0.05$) were considered non-significant and depicted with alphabets. Scale Bar=100 mm (a), 100 μm (c-h).

Supplementary Figure. 21

Cell death assay in *nac044-1*, *nac085-2,* and the double mutants with *med14-1* and *hy5*

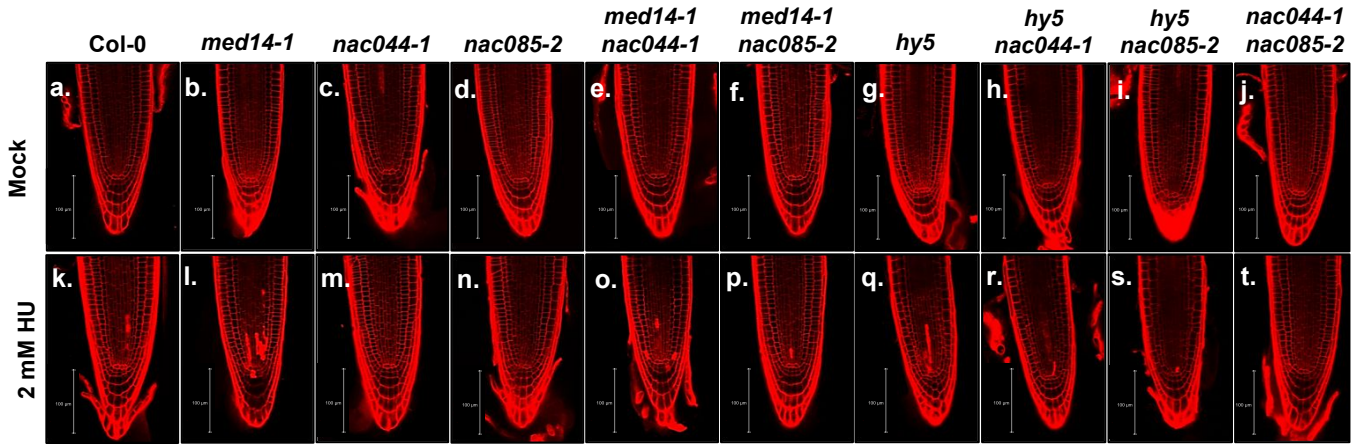

S21: Functional loss of NAC044 and NAC085 helps to partially rescue the cell death in *med14* and *hy5* under genotoxic stress. a-t, Confocal images showing the cellular damage in Col-0, *med14-1*, *hy5*, *nac044-1*, *med14-1 nac044-1*, *nac085-2*, *med14-1 nac085-2, hy5 nac044-1, hy5 nac085-2,* and *nac044-1 nac085-2* roots, treated with HU and stained with PI. Cellular damage was observed in the PI-stained roots. Red PI-stained blotches at the root tip denote cell death. Data shown in the bar graph represents the average of three independent biological replicates containing at least 15 seedlings. Scale bar = 100 μm.

Supplementary Figure. 22

HY5 transcriptionally suppresses the DDR response under oxidative stress

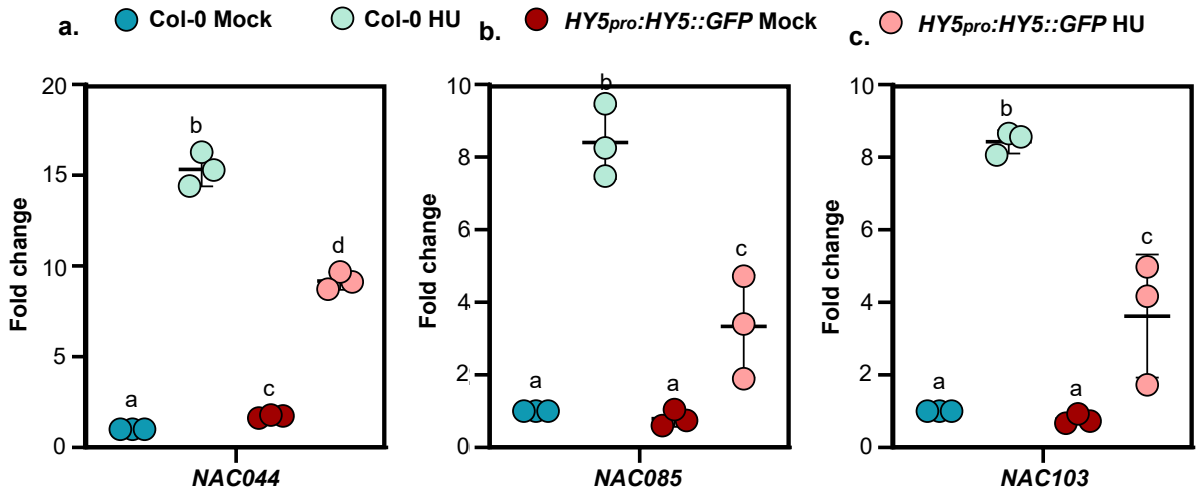

S22: HY5 negatively regulates transcription of *NAC044*, *NAC085,* and *NAC103*. a-c, Scattered dot plots showing the expression of *NAC044*, *NAC085,* and *NAC103* in root tissues of Col-0, *HY5$_{pro}$:HY5::GFP* after the mock and HU treatment respectively. Gene expression values were calculated as fold change ($2^{-\Delta\Delta CT}$). qRT-PCR analysis was performed with three independent biological replicates (n=3) and repeated the experiment twice. Gene expression was normalized from 18S, as a control. Scatter plots represent individual values of biological replicates and error bars denote standard deviation (SD). Statistical significance was determined using a one-way ANOVA followed by Tukey's honestly significant difference (HSD) post hoc test. Statistical significance was determined by a P-value of 0.05 or lower ($P \leq 0.05$), while P-values greater than 0.05 ($P > 0.05$) were considered non-significant and depicted with alphabets.

Supplementary Figure. 23

Binding of HY5 and MED14 on the promoter of *CYCD1;1* in response to HU

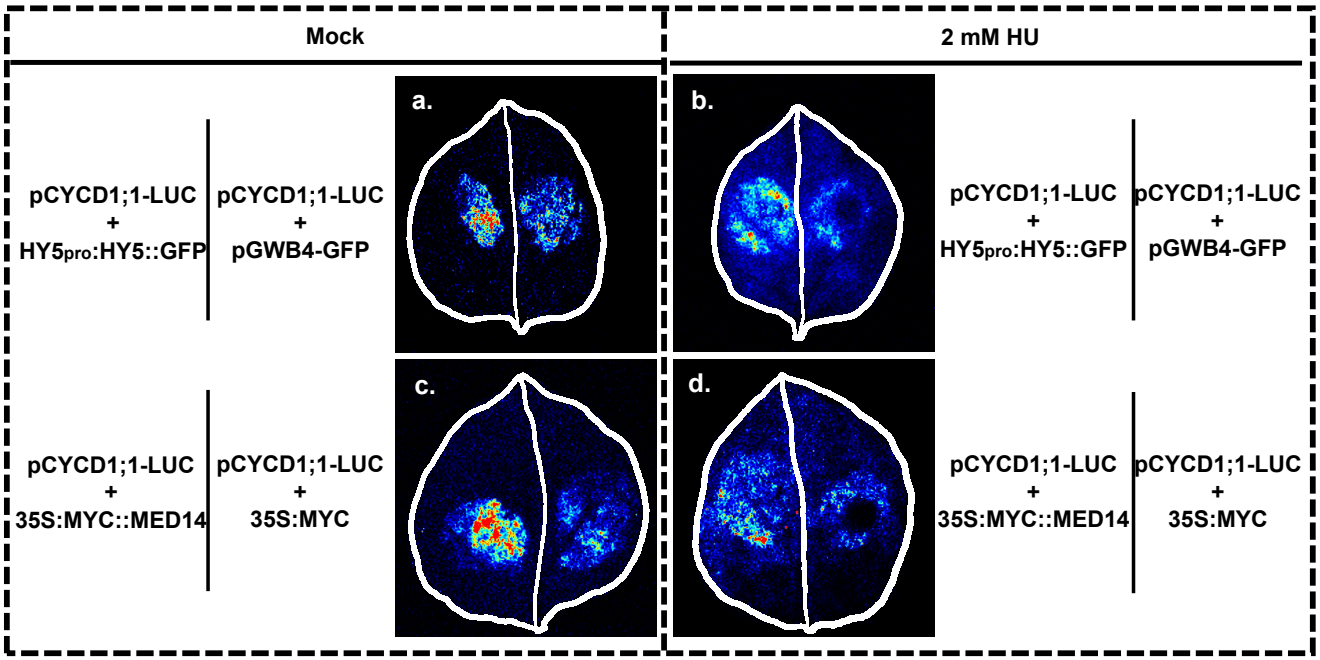

S23: MED14 and HY5 transcriptionally regulate *CYCD1;1* under genotoxic stress. Dual luciferase assay showing the activation of the promoter site of *CYCD1;1* by MED14 and HY5, in 6 h of mock and HU treatment. **a and b,** Binding of HY5 at *CYCD1;1* promoter; **c and d,** Binding of MED14 at *CYCD1;1* promoter.